

Optoacoustic study of nonlinear absorption of ultraviolet laser radiation by alkali-halide crystals during the generation of nonequilibrium carriers

B. G. Gorshkov, L. M. Dorozhkin, A. S. Epifanov, A. A. Manenkov, and A. A. Panov

Institute of General Physics, Academy of Sciences of the USSR

(Submitted 13 April 1984)

Zh. Eksp. Teor. Fiz. **88**, 21–29 (January 1985)

Comparison of laser photoconductivity data with measurements of nonlinear absorption in the ultraviolet range ($\lambda = 0.35$ and $0.27 \mu\text{m}$) is used to show experimentally that the principal mechanism of photoionization in chemically pure alkali-halide crystals at high illuminating intensities ($I \gtrsim 10^7 \text{ W/cm}^2$) is two-photon carrier production in the presence of their quadratic recombination. The optoacoustic method used to measure two-photon absorption combines simplicity of experimental technique with high reliability and sensitivity, and can be used in a wide range of intensities.

There has recently been considerable interest in studies of the absorption of optical radiation in very pure materials of different types, including wide-gap dielectric crystals. This has been dictated by the need to elucidate the mechanisms responsible for the absorption of radiation in different wavelength ranges (from the far infrared to the ultraviolet) in connection with the utilization of many wide-gap dielectrics as the working elements of high-power laser systems. Studies of intrinsic absorption mechanisms, due to the excitation of nonequilibrium carriers by powerful optical radiation as a result of collisional or multiphoton ionization of atoms in the main lattice of the crystal are of particular interest in the context.¹⁻⁴

Studies of the mechanisms responsible for the generation and recombination of nonequilibrium carriers in wide-gap dielectrics have attracted increasing attention in recent years. This is due, on the one hand, to the special role played by photoelectrons in the creation of radiation defects⁵⁻⁷ and, on the other hand, to the solution of problems on the limiting stability of transparent dielectrics under illumination by high-power laser radiation and the elucidation of mechanisms responsible for laser damage.

Many papers have been published on alkali-halide crystals (AHC) that are relatively widely used in laser optics, including the ultraviolet range. For example, Liu *et al.*⁸ used the photometric method to detect two-photon absorption by alkali-halide crystals of laser radiation at $\lambda = 0.35$ and $0.27 \mu\text{m}$, and have determined the corresponding two-photon absorption coefficients.

The creation and recombination of nonequilibrium carriers in chemically pure alkali-halide crystals was investigated experimentally by photoexcitation of electrons by ultraviolet laser radiation in Refs. 9 and 10, where the photoconductivity σ was measured as a function of the radiation intensity I , and the nature of this dependence was analyzed. The function $\sigma(I)$ was found to be nonlinear at $\lambda = 0.35 \mu\text{m}$ (Ref. 9) and at $\lambda = 0.35$ and $0.27 \mu\text{m}$ (Ref. 10) for $I \sim 10^5$ – 10^7 W/cm^2 . This nearly quadratic relationship was interpreted as two-photon (band-band) photoexcitation of carriers. At higher laser intensities ($I \sim 10^7$ – 10^8 W/cm^2), the function $\sigma(I)$ was found to change from quadratic to linear, and this was explained in Ref. 9 by the "turning on" of

the quadratic carrier recombination at these intensities, for which the recombination time is $\tau_p \sim N^{-1}$, where N is the free electron density.

Another possibility was also admitted in Ref. 10: the observed phenomena can be explained as the result of cascade excitation of carriers during transitions from the valence band of the crystals to the conduction band through stable intermediate levels of impurity or defect states. The attainment of the linear segment of the function $\sigma(I)$ at high laser intensities may then be due to the saturation of one of the cascade transitions.

The presence of quadratic carrier recombination was examined in Ref. 11, where a study of uv photon drag of nonequilibrium carriers in alkali-halide crystals, found experimentally, leads to the conclusion that this recombination occurred for $N \sim 10^{11}$ – 10^{12} cm^{-3} . However, the argument presented in Ref. 11 was incorrect.

Studies of the absorption of light can be used to distinguish quadratic carrier recombination during two-photon carrier creation (in which case, the absorbed energy is $E_{\text{abs}} \sim I^2$, and $\sigma \sim I$) from the saturation of one of the transitions in cascade ionization for which $E_{\text{abs}} \sim I$ and $\sigma \sim I$.

Moreover, for laser intensities for which quadratic recombination becomes appreciable, radiation defects are readily produced at the end of the laser pulse (see, for example, Refs. 5 and 9). In view of this, we have one further possible explanation of the change in the character of the function $\sigma(I)$ from quadratic to linear in the high-intensity region ($I \gtrsim 10^7 \text{ W/cm}^2$). This mechanism relies on the fact that the deep trapping (recombination) centers that appear under the influence of the ultraviolet radiation give rise to a more slowly-varying function $\sigma(I)$ because of the slower rise in carrier density.

The ionization of defects produced by powerful ultraviolet radiation (together with the trapping centers⁶) can then become more probable than electron-hole pairs created as a result of two-photon ionization.¹² The principal contribution to the absorption of laser radiation energy is then provided by ionization of recreated centers. This means that the absorbed energy can be a more rapidly-varying function of intensity as compared with the two-photon process for which $E_{\text{abs}} \sim I^2$.

Thus, the variation in the effective absorption coefficient may be a very useful source of information for the elucidation of the mechanisms responsible for the photoionization of wide-gap dielectrics by high-energy laser radiation.

The nature of optical absorption of energy that governs carrier dynamics is, in our view, best investigated by optoacoustic methods, which enable us to measure the integrated absorption within the body of a crystal and are therefore particularly appropriate for our purposes. We have therefore undertaken a detailed investigation of absorption in alkali-halide crystals at wavelengths corresponding to the third and fourth harmonics of the neodymium glass laser, using the optoacoustic method. We investigated crystals which we previously examined by the photoconductivity method.¹⁰ This enabled us to perform a correct comparison of the results and reliably interpret the photoexcitation and recombination of nonequilibrium carriers.

We note that the absorption of laser radiation by solids has been investigated by optoacoustic methods by many workers (see, for example, Refs. 13–15). The experimental technique is attractive because of its simplicity and reliability.

EXPERIMENT

We have studied the amplitude K of the acoustic wave produced when ultraviolet laser radiation is absorbed in alkali-halide crystals, as a function of the intensity of this radiation. Since we shall be concerned with intensities well below the threshold for laser damage within the body of the crystals,¹⁶ we may suppose that $A(I) \sim E_{\text{abs}}(I)$.

In our experiments, we used the third and fourth harmonics of a Q -switched Nd^{3+} :YAG laser ($\lambda = 0.35$ and $0.27 \mu\text{m}$, respectively), and carried out selection of transverse and longitudinal oscillation modes (the fundamental TEM_{00} mode was selected). The laser pulse length was 8 ns at half height, and the shape of the pulse was nearly Gaussian. The radiation energy was monitored in each burst, and was up to 50 mJ at $\lambda = 0.35$ and up to 10 mJ at $\lambda = 0.27$. The radiation intensity was reduced either in steps with the aid of filters, or continuously by reducing the laser pump energy.

The AHC specimens were chemically pure NaCl, KCl, and KBr single crystals in the form of parallelepipeds ($20 \times 20 \times 30 \text{ mm}$) with freshly cleaved surfaces. The specimens were first examined in a spectrophotometer in order to determine the initial absorption coefficient at the working wavelength. The experiment was continued long enough to acquire sufficient statistics for reliable interpretation (we examined 10–15 specimens of each AHC, using crystals obtained from different sources and grown by different methods).

The laser radiation was focused within the body of the AHC specimen by a quartz lens with a focal length $f \sim 400 \text{ mm}$. The laser-beam diameter near the front surface of the specimens was determined as described in Refs. 17 and 18, and was found to be about 1 mm at the $1/e$ level of maximum intensity along the laser beam axis. A 1-mm diameter stop was placed directly before the front surface of the specimen.

The laser intensities that we have used did not exceed

10^8 W/cm^2 , i.e., they were below the threshold for surface damage.¹⁹ All the same, we monitored the state of the surface of the specimens intercepting the laser radiation, as well as the absence of plasma on this surface under high-intensity illumination. The lower limit of the laser intensity used in our experiments was set by the sensitivity of the recording equipment, and was about 10^5 W/cm^2 .

The detector was a sensitive element made from the TsTS-19 piezoceramic. It was cylindrical in shape (diameter and height both equal to 2 mm) and, to improve acoustic matching, it was held against the surface of the specimens by a sound-absorbing medium. The sensitive element was mounted on the side surface of the specimen at a distance of 10 mm from the end surface through which the laser radiation was introduced. The distance between the detector and the laser-beam axis was about 10 mm. In this detector geometry, the signal due to the absorption of radiation by the front surface of the crystal appears *after* the signal due to the energy absorbed within the body of the crystal.

Steps were taken to exclude the influence on the detector of parasitic effects due to laser radiation scattering within the body of the crystal specimen. An aluminium foil, which is a good reflector in the ultraviolet, was placed between the piezoceramic and the specimen in order to reduce the direct effect of the scattered radiation on the detector. Good acoustic coupling was ensured by depositing a thin layer of glycerin on the side surface of the specimen at the point where it was in contact with the detector.

The useful acoustic signal due to the absorption of laser energy within the body of the crystal specimen was in the form of damped oscillations of varying polarity and complex shape (Fig. 1), the appearance of which was delayed relative to the beginning of the laser by an amount corresponding to the propagation of the sound wave from the laser-beam axis to the piezodetector. The amplitude of the acoustic signal was taken to be the amplitude of the first pulse arriving from the illuminated volume.

The signal from the piezodetector was amplified by an amplifier based on the 574 UD1-A microcircuit (sensitivity at least 10^{-4} V), whose output was applied to one of the channels of the S8-2 double-beam recording oscilloscope. The second channel was used to record the amount of energy incident on the specimen. This was done by diverting a fraction of this energy by means of a plane-parallel quartz plate onto a high-sensitivity pyroelectric photodetector.²⁰

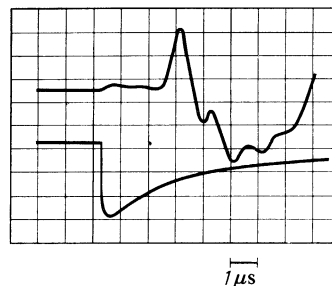


FIG. 1. Oscillogram of the acoustic signal (the lower trace is the laser pulse).

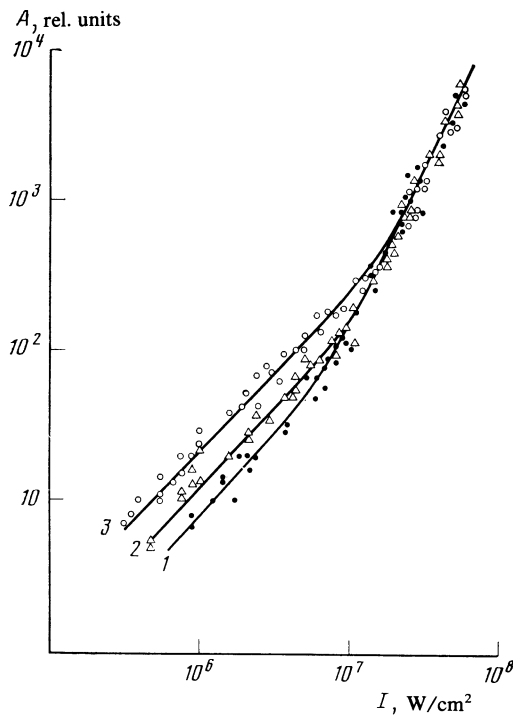


FIG. 2. Amplitude $A(I)$ of the acoustic signal for three specimens of KBr with different linear absorption coefficients ($\lambda = 0.35 \mu\text{m}$: 1— $\alpha = 0.04 \text{ cm}^{-1}$, 2— 0.07 cm^{-1} , 3— 0.12 cm^{-1}).

Since, in the interior of the AHC specimens, the laser beam was axially symmetric and only slightly attenuated along the length of the specimen (about 3–4 cm) because of the low absorption at these wavelengths,²¹ the acoustic wave generated within the crystal was cylindrically symmetric.

Our measurements of the amplitude of the acoustic signal (detector reaction time $\sim 1 \mu\text{s}$) were so arranged that the pressure on the piezodetector was proportional to the mean pressure P in the interior of the heated region. Since the heat released in the illuminated volume during the laser pulse is thermally conducted to a characteristic distance $l = (\tau_r \chi)^{1/2} \sim 2 \cdot 10^{-5} \text{ cm}$ (χ is the thermal diffusivity of the material), and since $l \ll d$ (d is the diameter of the laser beam, the absolute magnitude of T can be estimated from $P = \Gamma E_{\text{abs}}$ where $\Gamma = \gamma v^2 / C_V$ is the Grüneisen coefficient, γ is the temperature coefficient of thermal expansion, v is the velocity of sound in the material under investigation, and C_V is the specific heat of the material.

Since, even for the maximum laser intensity that we have used, the energy absorbed during the pulse is about 0.1 J/cm^3 , the above estimate yields $P \sim 3 \text{ bar}$. For sound-wave intensities corresponding to this pressure, the intrinsic ab-

sorption of sound by the crystal is essentially linear (in intensity). Changes in the medium density and sound-wave velocity under such pressures are small and can be neglected.²²

It was therefore expected that, under our conditions, there would be no linear distortions due to the transfer of acoustic-wave energy from the illuminated volume to the piezodetector whose sensitivity was independent of the pressure P throughout the laser intensity range under investigation. The linearity of the detector incorporating the optoacoustic probe was monitored by monitoring the function $A(I)$ in a broad range of intensities.

EXPERIMENTAL RESULTS

To compare the present results with those reported in Ref. 10, where the photoconductivity was measured as a function of the incident laser intensity at the same wavelength, we selected KBr crystals for measurements at $\lambda = 0.35 \mu\text{m}$. Figure 2 shows the amplitude $A(I)$ of the acoustic signal at $\lambda = 0.35 \mu\text{m}$ for three KBr crystals with different linear absorption coefficients α at this wavelength. The initial absorption coefficients of the AHC specimens at $\lambda = 0.35$ and $0.27 \mu\text{m}$, measured with the spectrophotometer, are listed in Table I.

Figure 2 shows that the $A(I)$ curve consists of two characteristic segments for all the KBr specimens that we investigated (we reproduce the results for specimens with maximum contrast in α): there is a linear segment at relatively low laser intensities ($I \sim 3 \times 10^5 - 8 \times 10^6 \text{ W/cm}^2$) and a quadratic segment at higher intensities ($I \sim 10^7 - 10^8 \text{ W/cm}^2$). Despite the considerable difference (by factors of more than three) in the values of α for these specimens, their absorption is practically the same in the high-intensity region.

Figure 3 shows the function $A(I)$ at $\lambda = 0.27 \mu\text{m}$ for two KCl crystal specimens with different initial absorption coefficients (see Table I). The band gap in KCl has been reliably measured and amounts to $\epsilon_g \sim 8.7 \text{ eV}$ (Ref. 23), so that the energy of the two quanta at the wavelength of the fourth harmonic of the neodymium laser is $2\hbar\omega_4 > \epsilon_g$. It is clear from Fig. 3 that the function $A(I)$ for KCl also exhibits two characteristic segments, namely, the linear segment for $I \sim 10^5 - 10^7 \text{ W/cm}^2$ and the quadratic segment for $I \gtrsim 10^7 \text{ W/cm}^2$. The initial absorption (which varies by facts of 2–2.5, judging by the amplitude of the acoustic signal) is replaced by practically equal absorption at high laser intensities.

Figure 4 shows the measured absorption functions at the wavelength of $0.27 \mu\text{m}$ for different AHC specimens with very similar linear absorption coefficients at this wave-

TABLE I. Linear absorption coefficients α of alkali-halide crystals, cm^{-1} .

Specimen	$\lambda=0,35 \mu\text{m}$	$\lambda=0,27 \mu\text{m}$	Specimen	$\lambda=0,35 \mu\text{m}$	$\lambda=0,27 \mu\text{m}$
NaCl	—	0,23	KBr-4	—	0,07
KBr-1	0,12	—	KCl-1	—	0,08
KBr-2	0,07	—	KCl-2	—	0,24
KBr-3	0,04	—			

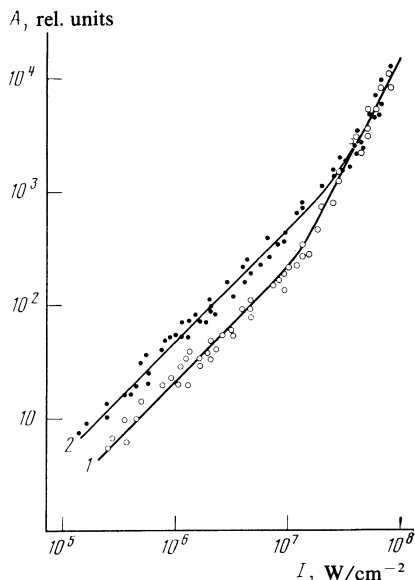


FIG. 3. Amplitude $A(I)$ of the acoustic signal for two specimens of KCl with different linear absorption coefficients ($\lambda = 0.27 \mu\text{m}$: 1— $\alpha = 0.08 \text{ cm}^{-1}$, 2— 0.24 cm^{-1}).

length (see the table). Whereas the curves practically overlap at relatively low intensities corresponding to the linear segment, they are well separated at high intensities [but the slope is the same and corresponds to the quadratic form of $A(I)$], indicating substantially different values of nonlinear absorption in this intensity range.

DISCUSSION OF EXPERIMENTAL RESULTS

Since the function $A(I)$ consists of two segments, namely, the linear segment at low intensities and the quadratic segment at high intensities, and this was confirmed for all our AHC specimens, these two segments are naturally attributable to different physical mechanisms of energy absorption within the body of the crystal.

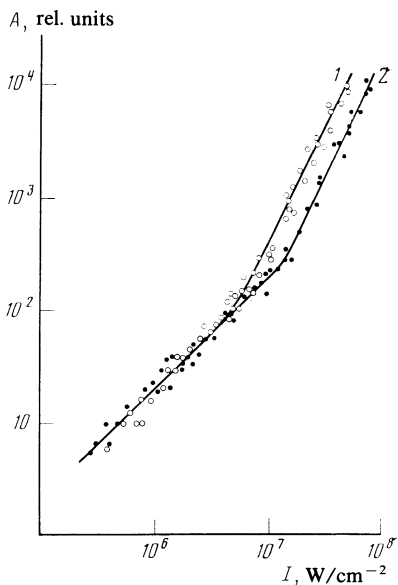


FIG. 4. Amplitude $A(I)$ of the acoustic signal for the following specimens ($\lambda = 0.27 \mu\text{m}$): 1—KBr ($\alpha = 0.07 \text{ cm}^{-1}$) and 2—KCl ($\alpha = 0.08 \text{ cm}^{-1}$).

The linear segment shows that a definite portion of the laser-beam energy is probably absorbed as a result of ionization of impurity states, which is linear in intensity, and that a considerable fraction of this energy is rapidly transferred to the crystal lattice. The appearance of the quadratic segment on the $A(I)$ curve at high intensities can be explained only by assuming that nonlinear absorption exceeds linear absorption, and the absorption coefficient becomes proportional to the intensity of the laser radiation. Precisely this situation should prevail in the case of two-photon (band-band) absorption of energy.

It is important to emphasize that we have investigated media with similar acoustic parameters (alkali-halide crystals), but that the specimens had appreciably different linear absorption coefficients. When the experimental data shown in Figs. 2 and 3 are analyzed, it is noticeable that, on the linear segment, the largest acoustic signal is observed for specimens with the largest value of α (and conversely).

As noted above, at high laser ultraviolet intensities, i.e., on the quadratic segment of the $A(I)$ curve, all the curves obtained for specimens of the same AHC become practically identical, whereas the initial amplitudes of the acoustic signals (for different α) are appreciably different. All this suggests that the nonlinear absorption of energy has an intrinsic character that is unrelated to impurity concentration in the specimens that we have investigated.

In addition, studies of the mechanisms responsible for the recombination of electron-hole pairs produced during two-photon absorption (see, for example, Refs. 6 and 9), which have been carried out by picosecond spectroscopy, have established that the interaction between radiation defects produced by powerful ultraviolet radiation ensures that a high percentage of the absorbed laser pulse energy is transferred to the lattice. For high concentrations of nonequilibrium carrier ($\sim 10^{15}$ – 10^{16} cm^{-3}), the process is intrinsic in character and is independent of the individual properties of the AHC specimens.

We may therefore conclude that the data obtained in this research show that, under the conditions of our experiments, we were dealing with two-photon absorption (band-band) and not the cascade ionization of impurities.

On the quadratic segment of the $A(I)$ function, the experimental curves obtained for different AHC do not overlap even when the initial absorption is the same (see Table I). This is illustrated in Fig. 4 in the case of KBr and KCl crystals.

Because of this, we have tried to estimate the two-photon absorption coefficient for different alkali-halide crystals. This estimate was made by matching the measured $A(I)$ to the measured linear absorption coefficient. We assumed that the magnitude of α for the AHC specimens remained constant for all laser intensities right up to the end of the linear segment of $A(I)$. Moreover, we assumed that a large proportion of the absorbed energy was transferred to the crystal lattice in a time much shorter than the response time of the piezodetector (about $1 \mu\text{s}$) for both single-photon and two-photon processes.

The estimated two-photon absorption coefficient β , obtained under the above assumptions for the AHC specimens,

TABLE II. Two-photon absorption coefficients β of alkali-halide crystals, 10^3 cm/MW.

Specimen	$\lambda=0,35 \mu\text{m}$	$\lambda=0,27 \mu\text{m}$	Specimen	$\lambda=0,35 \mu\text{m}$	$\lambda=0,27 \mu\text{m}$
NaCl	—	9,2	KBr-4	—	3,5
KBr-1	3,1	—	KCl-1	—	2,1
KBr-2	2,4	—	KCl-2	—	4,0
KBr-3	1,7	—			

are listed in Table II. We note that these values are very close to those reported in Ref. 8, where they were determined from the transmission of light at the same wavelength. The values of β for different specimens of the same AHC are seen to be somewhat different in our case because not all the laser radiation energy absorbed by the body of the crystal was released in the form of heat in a short interval of time. Some of the absorbed energy was expended in exciting luminescence centers and long-lived centers which stored it for a time exceeding the period of acoustic oscillations ($\approx 10^{-7}$ s). It is clear that the fraction of absorbed energy appearing in the form of heat, and responsible for the measured acoustic signal, may vary from specimen to specimen, depending on the concentration of particular defects and impurities.

Our previous data, obtained by laser photoconductivity¹⁰ at $\lambda = 0.35 \mu\text{m}$ for KBr and at $\lambda = 0.27 \mu\text{m}$ for NaCl, KCl, and KBr, showed the presence of a transition from the quadratic to the linear segment on the $\sigma(I)$ curve in the region of high laser intensities ($I \gtrsim 5 \cdot 10^6$ W/cm²). Comparison of these data with the optoacoustic measurements of absorption shows that, for the same intensities (and the same wavelengths), for which $A(I) \sim I^2$, the photoconductivity of the alkali-halide crystals is due to two-photon ionization and not to cascade processes. The slower variation in $\sigma(I)$ for $I \gtrsim 5 \cdot 10^6$ W/cm² (which corresponds to nonequilibrium carrier concentration $N \sim 10^{12} - 10^{13}$ cm⁻³, Ref. 10), i.e., replacing the quadratic with the linear variation, can be explained in this case only by the dominant influence of quadratic recombination.

¹N. Bloembergen, J. Quant. Electron. **QE-10**, 375 (1975).

²P. Bräunlich, A. Schmid, and P. Kelly, Appl. Phys. Lett. **26**, 150 (1975).

³P. Kelly, P. Bräunlich, and A. Schmid, Appl. Phys. Lett. **26**, 223 (1975).

⁴N. L. Boling, P. Bräunlich, A. Schmid, and P. Kelly, Appl. Phys. Lett. **27**, 191 (1975).

⁵J. N. Bradford, R. T. Williams, and W. L. Faust, Phys. Rev. Lett. **35**, 300 (1975).

⁶R. T. Williams, J. N. Bradford, and W. L. Faust, Phys. Rev. B **18**, 7038 (1978).

⁷M. N. Kabler and R. T. Williams, Phys. Rev. B **18**, 1948 (1978).

⁸P. Liu, S. W. Lee, H. Lotem, J. H. Bechtel, N. Bloembergen, and R. S. Adhav, Phys. Rev. B **17**, 4620 (1978).

⁹R. T. Williams, P. H. Klein, and C. L. Marquardt, NBS Spec. Publ. N 509, 1977, p. 481.

¹⁰V. G. Gorshkov, A. S. Epifanov, A. A. Manenkov, and A. A. Panov, Zh. Eksp. Teor. Fiz. **81**, 1423 (1981) [Sov. Phys. JETP **54**, 755 (1981)].

¹¹B. G. Gorshkov and A. A. Panov, Fiz. Tverd. Tela (Leningrad) **23**, 3597 (1981) [Sov. Phys. Solid State **23**, 2090 (1981)].

¹²A. S. Epifanov, A. A. Manenkov, A. A. Panov, and E. M. Shakhverdiev, Tezisy dokladov VI Vsesoyuznoi konferentsii po nerezonansnomu vzaimodeistviyu opticheskogo izlucheniya s veshchestvom (Abstracts of Papers read to the Sixth All-Union Conf. on Nonresonance Interaction of Optical Radiation with Matter), Vilnius, 1984, p. 190.

¹³A. Hordvic and H. Schlossberg, Appl. Opt. **16**, 101 (1977).

¹⁴C. B. Scruby, J. C. Collingwood, and H. N. G. Wadley, J. Phys. D: Appl. Phys. **11**, 2359 (1978).

¹⁵V. D. Valovik and S. I. Ivanov, Zh. Eksp. Teor. Fiz. **47**, 1565 (1977) [sic].

¹⁶B. G. Gorshkov, A. S. Epifanov, A. A. Manenkov, and A. A. Panov, Kvantovaya Elektron. (Moscow) **6**, 2415 (1979) [Sov. J. Quantum Electron. **9**, 1420 (1979)].

¹⁷W. L. Smith, J. H. Bechtel, and N. Bloembergen, Phys. Rev. B **12**, 706 (1975).

¹⁸D. R. Skinner and R. E. Witcher, J. Phys. E **5**, 237 (1972).

¹⁹Yu. K. Danileiko, A. A. Manenkov, A. M. Prokhorov, and V. Ya. Khaimov-Mal'kov, Zh. Eksp. Teor. Fiz. **58**, 31 (1970) [Sov. Phys. JETP **31**, 18 (1970)].

²⁰L. M. Dorozhkin, V. S. Doroshenko, et al., V. sb Impul'snaya fotometriya, Mashinostroenie, Leningrad, 1979, p. 64.

²¹N. V. Volkova, Fiz. Tverd. Tela (Leningrad) **16**, 307 (1974) [Sov. Phys. Solid State **16**, 59 (1974)].

²²F. F. Voronov, E. V. Chernysheva, and V. A. Goncharova, Fiz. Tverd. Tela (Leningrad) **21**, 100 (1979) [Sov. Phys. Solid State **21**, 59 (1979)].

²³E. D. Aluker, D. Yu. Lysis, and S. A. Chernov, Elektronnyye vzbuzhdeniya i radioluminestsentsiya shchelochno-galoidnykh kristallov (Electron Excitations and Radioluminescence of Alkali-Halide Crystals), Zinatne, Riga, 1979, p. 251.

Translated by S. Chomet